

Beyond the Child-Langmuir limit

R. E. Caflisch^{1,2} and M. S. Rosin¹

¹*Department of Mathematics, UCLA, Los Angeles, California 90095, USA*

²*Institute for Pure and Applied Mathematics, UCLA, Los Angeles, California 90095, USA*

(Received 21 July 2011; revised manuscript received 28 March 2012; published 18 May 2012)

This article presents a new formulation of the solution for fully nonlinear and unsteady planar flow of an electron beam in a diode. Using characteristic variables (i.e., variables that follow particle paths) the solution is expressed through an exact analytic, but implicit, formula for any choice of incoming velocity v_0 , electric field E_0 , and current J_0 . For steady solutions, this approach clarifies the origin of the maximal current J_{\max} , derived by Child and Langmuir for $v_0 = 0$ and by Jaffé for $v_0 > 0$. The implicit formulation is used to find (1) unsteady solutions having constant incoming flux $J_0 > J_{\max}$, which leads to formation of a virtual cathode, and (2) time-periodic solutions whose average flux exceeds the adiabatic average of J_{\max} .

DOI: [10.1103/PhysRevE.85.056408](https://doi.org/10.1103/PhysRevE.85.056408)

PACS number(s): 52.59.Sa

I. INTRODUCTION

Space-charge limiting (SCL) current is a fundamental constraint on the flow of an electron beam in a diode. For a fixed potential difference ϕ_1 and incoming velocity v_0 , the maximal sustainable steady-state current J_{\max} was derived by Child [1] and Langmuir [2] for $v_0 = 0$ and by Jaffé [3] for $v_0 > 0$. The physical origin of the SCL effect is clear: the electromotive force from electrons in the beam limits the current in the diode. If the incoming current is maintained above this maximum, then the electron density builds up inside the diode and a virtual cathode develops. The basic physics and technological applications of SCL flows and virtual cathodes are well reviewed in Refs. [4,5]. Extensions to more general physics and geometries have been carried out, mostly using perturbation methods or simulations, for example, Ref. [6] for multidimensional geometries.

The mathematical derivation of the maximal current in Refs. [1–3] is based on equations for the steady, one-dimensional electron flow in a diode. The authors derive a formula relating the current and the potential jump, but the analysis for $v_0 > 0$ in [3] is complicated. Simplified derivations for the maximal steady current, as well as stability analyses for electron-ion diode flows, were performed [7–11] through a Lagrangian formulation of the diode equations in terms of particle paths. A Lagrangian formulation was also used to show that formation of a virtual cathode is related to cusp formation in the electron trajectories [12–14] and to describe multivalued solutions [15].

This article presents a new formulation for the complete solution of the one-dimensional diode equations. The solution is based on a Lagrangian formulation (i.e., particle paths or characteristics) so that it is an extension of Refs. [7–11]. Our main result is an implicit solution that applies to both steady and unsteady flows and to the fully nonlinear equations with no approximations.

This implicit solution is analogous to the implicit solution for the inviscid Burgers equation (e.g., see Ref. [16]), since velocity v , density ρ , electric field ψ , and spatial position x are found through simple, explicit formulas in terms of characteristic variables s and τ . From this implicit formulation, it is straightforward to derive the maximal current that was first found in Refs. [1–3]. In addition, the implicit solution

formulation enables construction of unsteady solutions that exhibit important properties, including singularity formation corresponding to cusp formation in the characteristics and formation of a virtual cathode, and time-periodic solutions whose average flux exceeds the adiabatic average of J_{\max} .

The one-dimensional continuum equations for the flux of electrons in a diode are

$$\partial_t \rho + \partial_x(\rho v) = 0, \quad (1)$$

$$\partial_t v + v \partial_x v = \partial_x \phi, \quad (2)$$

$$\partial_x^2 \phi = \rho, \quad (3)$$

in which x , t , v , ϕ , and ρ are the scaled position, time, velocity, potential, and density given by

$$(x, t, v, \phi, \rho) = [x'/L, t'/T, v'/(L/T), \phi'/\Phi, \rho'/R],$$

$$\Phi = (m_e/q_e)(L/T)^2, \quad R = (\epsilon_0/q_e)(\Phi/L^2).$$

The primed variables are unscaled, L and T are length and time scales, m_e is the electron mass, q_e is the fundamental charge (positive), and ϵ_0 is vacuum permittivity. The boundary conditions at the cathode $x_0 = 0$ and anode $x_1 = d$ are

$$\left. \begin{aligned} \phi &= 0 \\ v &= v_0 \\ \rho &= \rho_0 \end{aligned} \right\} \text{ on } x = 0, \quad (4)$$

$$\phi = \phi_1 \text{ on } x = d.$$

so that ϕ_1 is the potential difference across the channel.

II. CHARACTERISTIC FORMULATION

Consider characteristic (particle-path) variables in which $x(s, \tau)$ is the position at time $t = s + \tau$ for a particle that entered the domain at time τ . The defining equations for s and τ are

$$\partial_s x = v, \quad (5)$$

$$x(0, \tau) = 0, \quad t = s + \tau. \quad (6)$$

Derivatives in (x, t) and in (s, τ) are related by

$$\partial_s = \partial_t + v \partial_x, \quad \partial_\tau = \partial_t + (\partial_\tau x) \partial_x. \quad (7)$$

Denote (scaled) negative electric field by $\psi = \partial_x \phi$ (since the electric field is $E = -\partial_x \phi$). Since $\partial_x \psi = \rho$, then $\psi(x, t)$ is the total mass between 0 and x , plus some boundary terms, which implies

$$\partial_t \psi + v \partial_x \psi = f''''(t) \quad (8)$$

for some function f'''' (the four derivatives are for notational convenience below). Combine Eq. (8) with Eqs. (2) and (5), using Eq. (7), to get the following system:

$$\partial_s \psi = f''''(s + \tau), \quad \partial_s v = \psi, \quad \partial_s x = v. \quad (9)$$

The general solution for this system, using Eq. (6), is

$$\begin{aligned} \psi(s, \tau) &= \theta(\tau) + f''''(s + \tau), \\ v(s, \tau) &= w(\tau) + \theta(\tau)s + f''(s + \tau), \\ x(s, \tau) &= w(\tau)s + \frac{1}{2}\theta(\tau)s^2 + f'(s + \tau) - f'(\tau). \end{aligned} \quad (10)$$

For notational convenience below, we also set

$$\begin{aligned} f''''(s + \tau) &= g'''(s + \tau) + (s + \tau)a_0, \\ \theta(\tau) &= \gamma(\tau) - a_0\tau + \gamma_0, \end{aligned} \quad (11)$$

in which a_0 and γ_0 are constants. The system (10) provides a new general method for solving the unsteady diode Eqs. (1)–(3).

In Eq. (10) f , θ , and w are related to boundary data by

$$f'''' = \partial_\tau \psi_0 + J_0, \quad \theta = \psi_0 - f''', \quad w = v_0 - f'',$$

in which $J_0 = \rho_0 v_0$ and $\psi_0 = \psi(x = 0)$ are incoming flux and negative electric field. Specification of boundary data on $x = d$ requires identification of the crossing time $s = T(\tau)$ at which characteristics (particle paths) hit $x = d$; that is,

$$x(T(\tau), \tau) = d. \quad (12)$$

The density, flux, and potential satisfy (using $\partial_x = (v - \partial_\tau x)^{-1}(\partial_s - \partial_\tau)$ and $\partial_\tau x = 0$ at $x = 0$)

$$\rho = (v - \partial_\tau x)^{-1}(\partial_s - \partial_\tau)\psi, \quad (13)$$

$$J = v(v - \partial_\tau x)^{-1}(\partial_s - \partial_\tau)\psi,$$

$$J_0 = (\partial_s - \partial_\tau)\psi(0, \tau),$$

$$(\partial_s - \partial_\tau)\phi = (v - \partial_\tau x)\psi. \quad (14)$$

Equation (14) can be integrated (using $\phi(0, \tau) = 0$) to get

$$\phi(s, \tau) = \int_0^s (v - \partial_\tau x)\psi(s', \tau + s - s') ds'. \quad (15)$$

III. STEADY SOLUTIONS

Next we consider steady solutions, which cannot depend on τ , so that $f'''' = J_0$ is a constant, and the resulting solutions of system (9), using the variables of (11) with $\gamma_0 = \psi_0$, $a_0 = J_0$, and $\gamma = g = 0$, are

$$\begin{aligned} \psi(s) &= \psi_0 + J_0 s, \\ v(s) &= v_0 + \psi_0 s + J_0 s^2/2, \\ x(s) &= v_0 s + \psi_0 s^2/2 + J_0 s^3/6, \\ \phi(s) &= \frac{1}{2}[v(s)^2 - v_0^2]. \end{aligned} \quad (16)$$

In particular, the value ϕ_1 of the potential at $x = d$ is

$$\phi_1 = \frac{1}{2}[v(T)^2 - v_0^2] = \frac{1}{2}(v_0 + \psi_0 T + \frac{1}{2}J_0 T^2)^2 - \frac{1}{2}v_0^2. \quad (17)$$

This is equivalent to formulas derived in Refs. [1–3, 7, 11]. They showed that there is maximal value J_{\max} of the current for a given value of the potential difference ϕ_1 or, equivalently, that there is a minimal value ϕ_{\min} of the potential difference ϕ_1 for a given value of the incoming current J_0 .

The characteristic solution Eq. (16) shows that there is a solution of the diode equations for any choice of the mathematically natural boundary data v_0 , J_0 , and ψ_0 . The reason for the minimal potential jump ϕ_{\min} (or equivalently the maximal current J_{\max}) is that ϕ_1 has a minimum value as a function of ψ_0 , for fixed values of velocity v_0 and current J_0 .

To find this minimum value, first calculate $\partial_{\psi_0} T$ and $\partial_{\psi_0} \phi_1$ by differentiating the equation $v_0 T + \psi_0 T^2/2 + J_0 T^3/6 = d$ and Eq. (17) with respect to ψ_0 to get

$$\partial_{\psi_0} T = -\frac{1}{2}v(T)^{-1}T^2 \quad \partial_{\psi_0} \phi_1 = T(v_0 + \frac{1}{2}\psi_0 T).$$

The minimal value of ϕ_1 occurs when $\partial_{\psi_0} \phi_1 = 0$, which implies

$$\psi_0 = -2v_0 T^{-1}, \quad d = J_0 T^3/6.$$

At this value of T , the potential difference $\phi_1 = \phi_{\min}$ and current $J_0 = J_{\max}$ are

$$\begin{aligned} \phi_{\min} &= -\frac{1}{2}v_0(36d^2 J_0)^{1/3} + \frac{1}{8}(36d^2 J_0)^{2/3}, \\ J_{\max} &= \frac{2}{9}d^{-2}(v_0 + \sqrt{v_0^2 + 2\phi_1})^3, \end{aligned} \quad (18)$$

in which J_{\max} is Child-Langmuir space-charge limited current for a one-dimensional (1D), planar diode (as a function of the incoming velocity v_0 and potential jump ϕ_1). This expression was derived by Jaffe [3] using a nonzero value of v_0 to avoid an infinite electron density at the minimum of the potential as found in simpler derivations of Child and Langmuir [1, 2], which used $v_0 = 0$. Furthermore, ϕ_{\min} is the corresponding minimum value of the potential jump ϕ_1 for given values of the incoming velocity v_0 and the (incoming) current J_0 . Note the ϕ_{\min} is just the inverse function for J_{\max} as a function of ϕ_1 ; that is, $J_{\max}(v_0, \phi_{\min}(v_0, J_0)) = J_0$.

Finally, under the assumptions $v_0 > 0$ and $\phi_1 > 0$, we show that $-\sqrt{2v_0 J_0} < \psi_0$ is the allowable parameter set for steady solutions. Allowable solutions are those for which the velocity is always positive (i.e., $v(s) > 0$ for $0 < s < T$) since otherwise the particle paths are crossing and the model breaks down.

To show this, note v is quadratic in s , with minimum at $s = s_* = -\psi_0/J_0$ at which $v(s_*) = v_0 - \frac{1}{2}J_0^{-1}\psi_0^2$. The assumption that $\phi_1 > 0$ implies that $v(T) > v_0$, which is equivalent to $-J_0 T/2 < \psi_0$. If $\psi > 0$, then $s_* < 0$ and $v_0 = v(0) > 0$ implies that $v(s) > 0$ for $0 \leq s \leq T$. If $-J_0 T/2 < \psi_0 < 0$, then $0 < s_* < T$ so that $v(s) > 0$ for all $0 < s < T$ if and only if $v(s_*) > 0$, which is true if and only if $\psi_0 > -\sqrt{2v_0 J_0}$. It follows that the allowable set of values of ψ_0 is $-\sqrt{2v_0 J_0} < \psi_0$. These results are consistent with but more easily stated than those of Refs. [3, 11].

IV. SOLUTIONS WITH CONSTANT INCOMING VELOCITY AND FLUX

A. Simplified formulas for the implicit solution

Consider unsteady solutions having constant incoming velocity v_0 and flux J_0 . The implicit solution, using the variables of Eqs. (11) with $a_0 = J_0$ and $\gamma = 0$, then has the form

$$\begin{aligned}\psi(s, \tau) &= \gamma_0 + J_0 s + g'''(s + \tau), \\ v(s, \tau) &= v_0 + \gamma_0 s + J_0 \frac{1}{2} s^2 + g''(s + \tau) - g''(\tau), \\ x(s, \tau) &= v_0 s + \frac{1}{2} \gamma_0 s^2 + J_0 \frac{1}{6} s^3 + g'(s + \tau) - g'(\tau) - g''(\tau)s.\end{aligned}\quad (19)$$

The resulting potential ϕ is

$$\begin{aligned}\phi(s, \tau) &= [\gamma_0 + g'''(s + \tau)]x(s, \tau) + p_3(s) - d\gamma_0 \\ &\quad + 2J_0[-g(\tau) + g(\tau + s) - sg'(\tau) - \frac{1}{2}s^2g''(\tau)],\end{aligned}$$

in which p_3 is defined by Eq. (21). At $s = T(\tau)$, the equations for $\phi_1(\tau) = \phi(T, \tau)$ and $T(\tau)$ become

$$\begin{aligned}\phi_1(\tau) &= dg_+''' + p_3(T) + 2J_0(-g + g_+ - Tg' - \frac{1}{2}T^2g''), \\ d &= p_1(T) + g_+' - g' - g''T,\end{aligned}\quad (20)$$

in which

$$\begin{aligned}p_1(T) &= v_0 T + \gamma_0 \frac{1}{2} T^2 + J_0 \frac{1}{6} T^3, \\ p_3(T) &= d\gamma_0 + J_0(v_0 \frac{1}{2} T^2 + \gamma_0 \frac{1}{3} T^3 + J_0 \frac{1}{8} T^4), \\ g &= g(\tau), \quad g_+ = g(\tau + T).\end{aligned}\quad (21)$$

B. Stability analysis for steady solutions

As described in Sec. III, the steady state has $\gamma_0 = \psi_0$, $g = 0$ and ϕ_1 constant. It follows that the linearization of Eq. (20) about a steady-state solution is

$$\begin{aligned}dg_{1+}''' + 2J_0(g_{1+} - g_1 - T_0g_1' - \frac{1}{2}T_0^2g_1'') + p_3'(T_0)T_1 &= 0, \\ p_1'(T_0)T_1 - g_1'T_0 + g_{1+}' - g_1' &= 0,\end{aligned}\quad (22)$$

in which T_1 and g_1 are the perturbations around the steady-state values T_0 and $g_0 = 0$, and $g_{1+}'(\tau) = g_1'(\tau + T_0)$. Solve for T_1 from the second equation in Eq. (22) and substitute it into the first equation, using the definitions of p_1 and p_3 from Eq. (21), to obtain

$$0 = dg_{1+}''' + 2J_0(g_{1+} - g_1 - \frac{1}{2}T_0g_1' - \frac{1}{2}T_0^2g_1''). \quad (23)$$

Now look for a mode of the form $g_1 = \hat{g}_1 e^{\lambda\tau/T_0}$. The resulting dispersion curve is given by

$$1 - \tilde{d} = z(\lambda), \quad (24)$$

in which

$$\begin{aligned}z(\lambda) &= 12\lambda^{-3}[1 - \frac{1}{2}\lambda - e^{-\lambda}(1 + \frac{1}{2}\lambda)] + 1, \\ d &= \frac{1}{6}J_0T_0^3\tilde{d}.\end{aligned}\quad (25)$$

The result, Eq. (24), is equivalent to the dispersion relation found by Lomax [17] and by Kolinsky and Schamel [11] using a Lagrangian approach, which differs from the implicit solution approach used here. As found numerically by Sun and Rosin [18], Eq. (24) has exactly one solution λ for every $0 < \tilde{d} < 1$ and it is positive (i.e., nonoscillatory, unstable

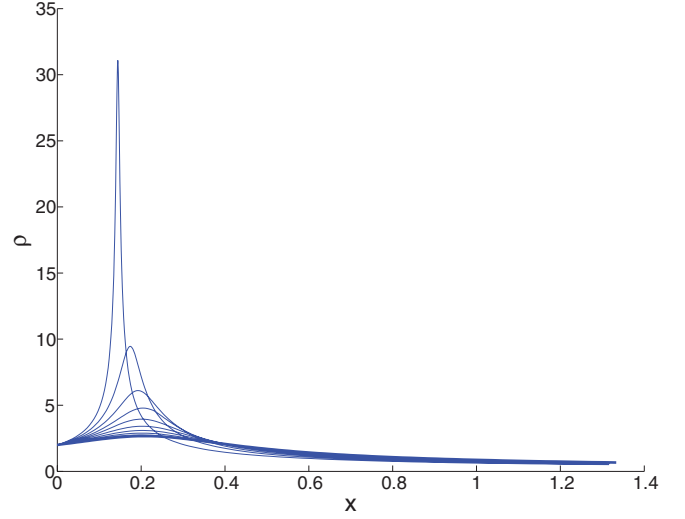


FIG. 1. (Color online) The density ρ for steady boundary data for which $J_0 > J_{\max}$. Values of ρ are presented at 11 times starting at $t = 0$ and ending at $t = 4$ with intervals $dt = 0.4$. Near $x = 0.2$ the value of ρ becomes singular as t increases.

mode). This corresponds to the linear instability of what is known in the literature as the “C-overlap flow.” For $\tilde{d} > 1$ all solutions have $\text{Re}(\lambda) < 0$. In the limiting case $\tilde{d} = 0$, there are a discrete set of pure imaginary solutions $\lambda = i\kappa$. Although these have no direct physical meaning for the linear problem, they could be meaningful for nonlinear solutions. In summary, the steady-state solution for the Child-Langmuir system is stable if and only $\tilde{d} > 1$, which is equivalent to the condition

$$\psi_0 > -2v_0/T_0 \quad (26)$$

found by Refs. [3,11].

C. Solutions with cusp formation

For a given function ϕ_1 , we solved the system Eq. (20) for $g(\tau)$ and $T(\tau)$ as a delay-differential equation, using the MATLAB routine *ddesd*, after some transformation to convert it into standard form for which the delays are backward. This amounts to solving for incoming electric field ψ for given values of the potential difference ϕ_1 .

We present numerical results for a solution that starts in the steady state \bar{F} with $(\bar{v}_0, \bar{J}_0, \bar{\phi}_1) = (0.5, 1, 1)$ on a system with thickness $d = 4/3$ (and with $\bar{\psi}_0 = -0.5$), for $t < 0$. This steady state is critical in that the potential difference is at its minimum (i.e., $\phi_1 = \phi_{\min}$) and the flux is at its maximum (i.e., $J_0 = J_{\max}$). The potential ϕ_1 varied linearly over the time interval $0 < t < 2$ up to the value $\tilde{\phi}_1 = \bar{\phi}_1 - 0.2$ and then is held constant at this value. Since this decreases the value of the potential jump ϕ_1 , the solution is not steady.

The resulting density ρ is presented in Fig. 1, which shows development of a singularity. Nevertheless, the function f''' remains smooth and bounded, so that implicit solution formulation remains valid up to the time of singularity formation. Characteristics are shown in Fig. 2, which shows formation of a caustic. Note that the velocity becomes negative before the cusp singularity.

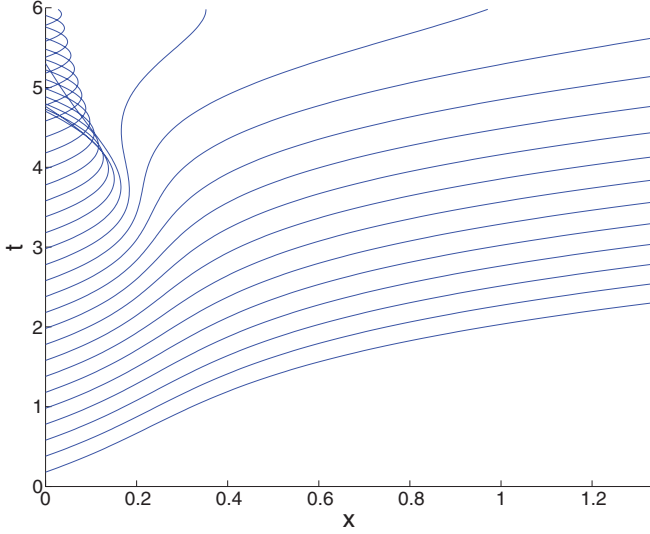


FIG. 2. (Color online) Characteristics (i.e., particle paths) for steady boundary data for which $J_0 > J_{\max}$. The solution breaks down when there is a cusp in the characteristics.

V. PERIODIC SOLUTIONS THAT EXCEED THE CHILD-LANGMUIR LIMIT ON AVERAGE

As a second example, consider unsteady solutions having constant incoming velocity v_0 but periodic flux $J_0(\tau)$ and periodic incoming electric field $\psi_0(\tau)$. The implicit form of the solution Eq. (9), using the variables in Eq. (11), is given by

$$\begin{aligned} \psi(s, \tau) &= \gamma_0 + \gamma(\tau) + a_0 s + g'''(s + \tau), \\ v(s, \tau) &= v_0 + \gamma_0 s + \gamma(\tau)s + a_0 \frac{1}{2}s^2 + g''(s + \tau) - g''(\tau), \\ x(s, \tau) &= v_0 s + \frac{1}{2}\gamma_0 s^2 + \frac{1}{2}\gamma(\tau)s^2 + a_0 \frac{1}{6}s^3 \\ &\quad + g'(s + \tau) - g'(\tau) - g''(\tau)s, \end{aligned} \quad (27)$$

in which γ and g are prescribed periodic functions.

We set

$$g(\tau) = g_1 \sin(k\tau), \quad \gamma(\tau) = \gamma_1 \sin(k\tau + \tau_1),$$

with period $P = 2\pi/k$. The incoming flux is

$$J_0(\tau) = a_0 - \gamma'(\tau).$$

For given values of the constants $v_0, \gamma_0, a_0, g_1, k, \gamma_1$, and τ_1 , the solution is constructed numerically: First, the crossing time $T(\tau)$ is found by solving Eq. (12) and the potential $\phi_1 = \phi(T(\tau), \tau)$ is found by numerical computation of the integral Eq. (15); that is,

$$\phi_1(\tau) = \int_0^{T(\tau)} (v - \partial_\tau x) \psi(s', \tau + T(\tau) - s') ds'$$

for a discrete set of values of τ . Second, the mean average incoming current \bar{J}_0 , the adiabatic average of the maximal current \bar{J}_{\max} , and their difference J_{diff} are defined as

$$\begin{aligned} \bar{J}_0 &= P^{-1} \int_0^P J_0(\tau) d\tau = a_0, \\ \bar{J}_{\max} &= P^{-1} \int_0^P J_{\max}(\tau) [1 + T'(\tau)] d\tau, \\ J_{\text{diff}} &= \bar{J}_0 - \bar{J}_{\max}. \end{aligned}$$

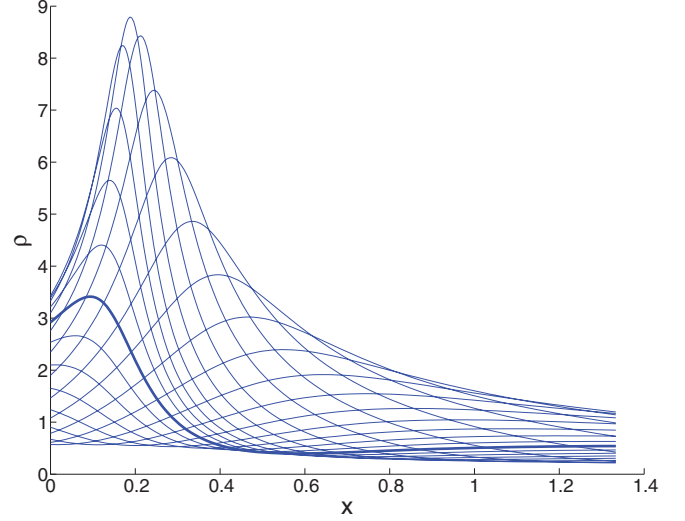


FIG. 3. (Color online) The density ρ at various times for periodic boundary data for which $\bar{J}_0 > \bar{J}_{\max}$. Values of ρ are presented at 21 times starting at $t = 0$ (bold curve) and at intervals of $dt = 0.161$. The highest value of ρ occurs at approximately $t = 0.8$, the time of bunching of characteristics in Fig. 4.

in which $J_{\max}(\tau)$ is defined by Eq. (18) using $\phi_1 = \phi_1(\tau)$. Note that \bar{J}_0 is averaged over $s = 0$ (i.e., $x = 0$) where $dt = d\tau$ and \bar{J}_{\max} is averaged over $s = T(\tau)$ (i.e., $x = d$) where $dt = [1 + T'(\tau)]d\tau$. Note that for a periodic flow, the average current is independent of the spatial position at which the average is performed. On the other hand, J_0 is the incoming current that is specified at $x = 0$ and ϕ_1 (the variable in J_{\max}) is the potential jump, which we think of as defined at $x = d$.

The adiabatic average is the pseudo-steady-state average that occurs in the asymptotic regime where $P \gg T$, so that average flux \bar{J}_{\max} can be achieved (at least in principle) by slowly varying the boundary conditions. Moreover, J_{\max} is a convex function, so that $J_{\max}(\bar{v}_0, \bar{\phi}_1) < \bar{J}_{\max}$, in which \bar{v}_0 and $\bar{\phi}_1$ are the mean averages of v_0 and ϕ_1 . These are the reasons that we compare \bar{J}_0 to \bar{J}_{\max} .

Solutions with $J_{\text{diff}} > 0$ (i.e., that exceed the Child-Langmuir limit on average) were found by Monte Carlo search over the values of the parameters k, γ_1 , and τ_1 . Results are shown below for $(v_0, a_0, \gamma_0, g_1, k, \gamma_1, \tau_1) = (0.5, 1, -0.5, 0.1, 1.949, 0.368, 2.268)$ on a system with thickness $d = 4/3$. In unscaled variables, the ratio of the potential energy difference across the domain (i.e., $q_e \phi_1'$) to the kinetic energy of incoming particles ($\frac{1}{2} m_e v_0^2$) is approximately 6.5 corresponding, for example, to 100 eV electrons entering into a 0.65 kV potential jump. The density ρ and characteristics are presented in Figs. 3 and 4. The resulting average values are $\bar{J}_0 = 1$ and $\bar{J}_{\max} = 0.8503$, so that $J_{\text{diff}} = 0.1497$ and the average incoming current \bar{J}_0 exceeds the adiabatic average of the maximal current \bar{J}_{\max} by about 17%.

Recent work [19] presents evidence that the average flux cannot exceed J_{\max} , under additional constraints that $v_0 = 0$ and that ϕ_1 is constant. However, there are experimental and numerical results showing that short, and even single-electron, current pulses can exceed the Child-Langmuir limit, and

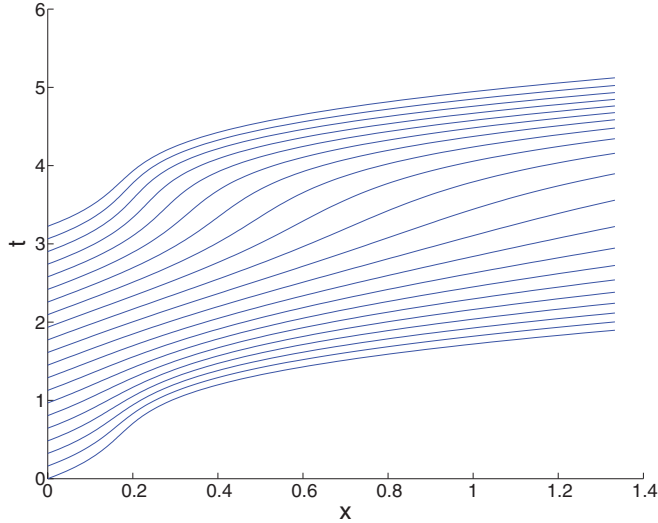


FIG. 4. (Color online) Characteristics (i.e., particle paths) for periodic boundary data for which $\bar{J}_0 > \bar{J}_{\max}$. Note that a cusp nearly forms in the characteristics.

periodic oscillations in the electron density at the cathode are a signature of a large potential difference across the domain [20–23]. Both effects may be related to the results found here.

VI. CONCLUSIONS

The unsteady solutions constructed above suggest that the implicit solution formulation may be useful for exploring additional properties of the diode equations, such as solutions that maximize the electric field strength and control methods to prevent formation of virtual cathodes.

ACKNOWLEDGMENTS

The authors thank John Luginsland, Andrew Christlieb, and Jean-Luc Cambier for numerous conversations and encouragement. Research was supported in part by the Air Force Office of Scientific Research STTR program through Grant No. FA9550-09-C-0115 and by the Department of Energy through Grant No. DE-FG02-05ER25710.

-
- [1] C. D. Child, *Phys. Rev. Series I* **32**, 492 (1911).
 - [2] I. Langmuir, *Phys. Rev.* **2**, 450 (1913).
 - [3] G. Jaffé, *Phys. Rev.* **65**, 91 (1944).
 - [4] C. K. Birdsall and W. B. Bridges, *Electron Dynamics of Diode Regions* (Academic Press, New York, 1966).
 - [5] R. B. Miller, *An Introduction to the Physics of Intense Charged Particle Beams* (Plenum, New York, 1982).
 - [6] J. W. Luginsland, Y. Y. Lau, R. J. Ulmstätt, and J. J. Watrous, *Phys. Plasmas* **9**, 2371 (2002).
 - [7] P. V. Akimov *et al.*, *Phys. Plasmas* **8**, 3788 (2001).
 - [8] B. B. Godfrey, *Phys. Fluids* **30**, 1553 (1987).
 - [9] W. S. Lawson, *Phys. Fluids B: Plasma Phys.* **1**, 1483 (1989).
 - [10] H. Schamel and V. Maslov, *Phys. Rev. Lett.* **70**, 1105 (1993).
 - [11] H. Kolinsky and H. Schamel, *J. Plasma Phys.* **57**, 403 (1997).
 - [12] E. A. Coutias, *J. Plasma Phys.* **31**, 313 (1984).
 - [13] E. A. Coutias, *J. Plasma Phys.* **40**, 369 (1988).
 - [14] E. A. Coutias and D. J. Sullivan, *Phys. Rev. A* **27**, 1535 (1983).
 - [15] X. Li, J. G. Wohlbiel, S. Jin, and J. H. Booske, *Phys. Rev. E* **70**, 016502 (2004).
 - [16] P. D. Lax, *Hyperbolic Systems of Conservation Laws and the Mathematical Theory of Shock Waves* (SIAM, Philadelphia, 1987).
 - [17] R. J. Lomax, *Proc. IEEE, Pt. C* **108**, 119 (1961).
 - [18] H. Sun and M. S. Rosin (unpublished).
 - [19] M. E. Griswold, N. J. Fisch, and J. S. Wurtele, *Phys. Plasmas* **17**, 114503 (2010).
 - [20] A. Valfells, D. W. Feldman, M. Virgo, P. G. O'Shea, and Y. Y. Lau, *Phys. Plasmas* **9**, 2377 (2002).
 - [21] Y. Zhu and L. K. Ang, *Appl. Phys. Lett.* **98**, 051502 (2011).
 - [22] A. Pedersen, A. Manolescu, and A. Valfells, *Phys. Rev. Lett.* **104**, 175002 (2010).
 - [23] M. E. Griswold, N. J. Fisch, and J. S. Wurtele, *Phys. Plasmas* **19**, 024502 (2012).